Supporting Information

Fine-tuning and electronic modulation of AuPdCu nanoflowers assembled with nanowires for robust ethanol oxidation reaction performance

Shengjun Zhang,[a,1] Jingzhou Liu,[a,1] Zhaochun Xu,[a] Dongfei Li,[b] Yue Cheng,[a,*] Xiaojun Zeng[a,*]

[a] Advanced Ceramic Materials Research Institute, School of Materials Science and Engineering, Jingdezhen Ceramic University, Jingdezhen 333403, China

[b] Yantai Aorun Energy Technology Co., Ltd., YanTai 265503, China

* Corresponding author, E-mail: 001025@jcu.edu.cn (Y. Cheng), zengxiaojun@jcu.edu.cn (X.J. Zeng)

[1] These authors contributed equally to this work.

1. DFT calculation method

All the density functional theory (DFT) calculations were carried out with the Vienna ab initio simulation package (VASP) code. To represent the electron-ion interactions, the Projector augmented wave (PAW) potentials were employed, and the Perdew-Burke-Ernzerhof (PBE) functional within the generalized gradient approximation (GGA) was adopted to describe the electron exchange-correlation interactions. The cutoff energy was set to 500 eV, and the convergence criteria for energy and force were 10^{-5} eV and 0.02 eV·$Å^{-1}$, respectively. During slab models construction, 15 Å vacuum space was adopted to reduce the influence of adjacent images. For all the calculations of slab models, a K-spacing value of 0.04 was used to generate K-Mesh. The dispersion-corrected DFT-D3 method was used to describe the van der Waals (vdW) interactions.

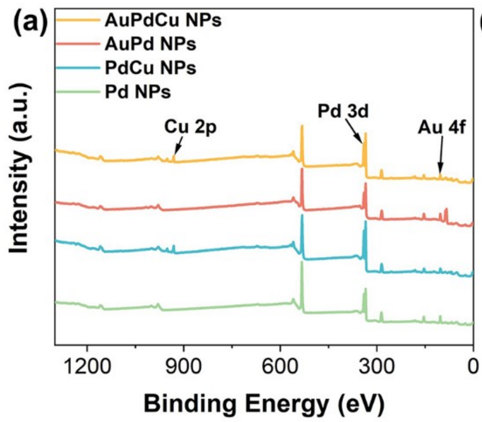

(b)

Catalysts	Au:Pd:Cu (atomic ratio)
AuPdCu NPs	11:80:9
AuPd NPs	13:87:0
PdCu NPs	0:85:15
Pd NPs	0:100:0

Fig. S1. (a) XPS survey spectra of the catalysts. (b) The contents of the elements obtained from ICP testing.

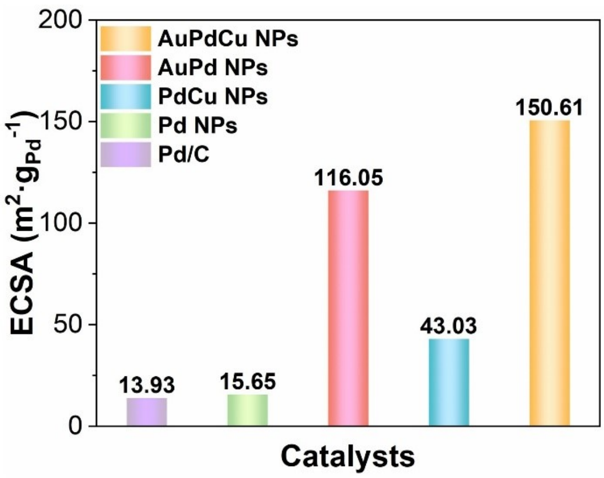

Fig. S2. ECSA values of the catalysts obtained from the CV curves collected in 1 M KOH.

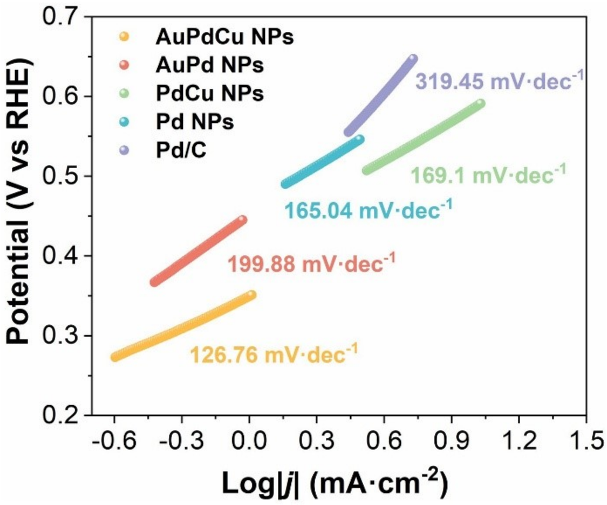

Fig. S3. Tafel plots of the catalysts obtained from the LSV curves.

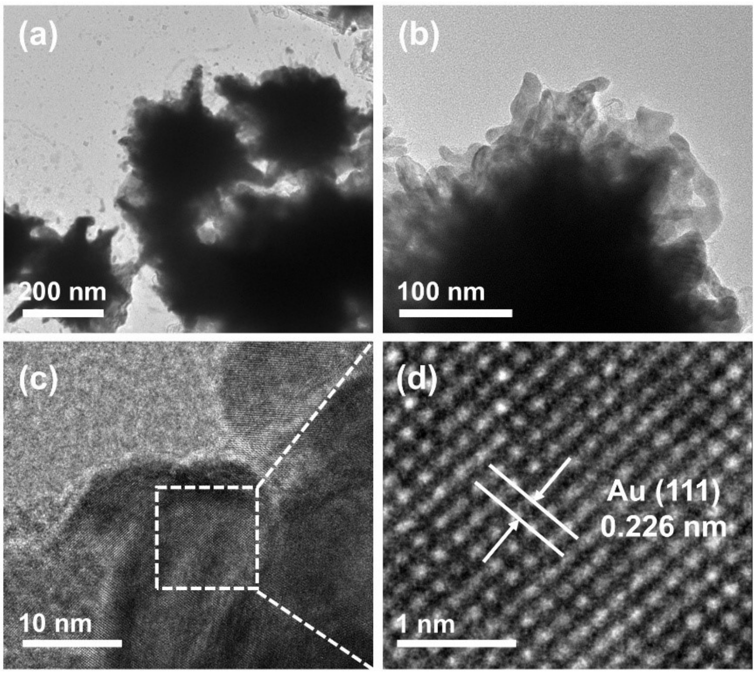

Fig. S4. (a,b) TEM and (c,d) HRTEM images of AuPdCu NPs after stability test.

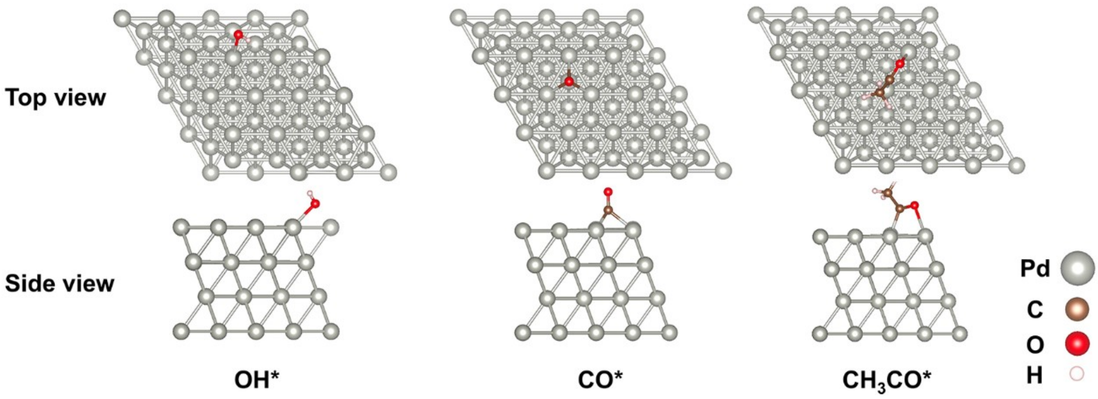

Fig. S5. Adsorption models of OH*, CO*, and CH_3CO* on Pd NPs.

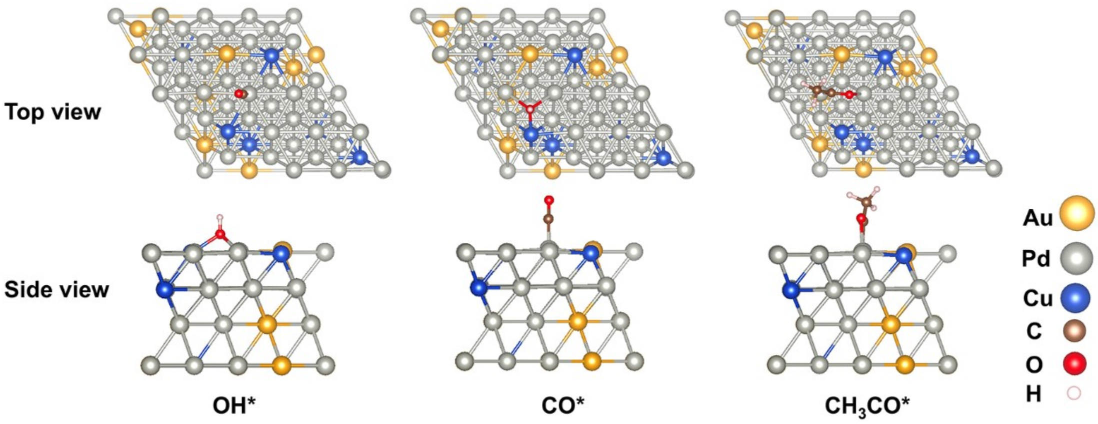

Fig. S6. Adsorption models of OH*, CO*, and CH_3CO* on AuPdCu NPs.

Table S1. Detailed XRD analysis of AuPdCu NPs and AuPd NPs.

Samples	**(111) 2θ (degree)**	**(111) Interplanar spacing (Å)**	**Au-Au bond length (Å)**	**Lattice strain (%)**
AuPdCu NPs	38.271	2.353	2.8826	-0.02
AuPd NPs	38.202	2.354	2.8834	0

Table S2. Detailed XRD analysis of PdCu NPs and Pd NPs.

Samples	**(111) 2θ (degree)**	**(111) Interplanar spacing (Å)**	**Pd-Pd bond length (Å)**	**Lattice strain (%)**
PdCu NPs	40.528	2.224	2.7237	-0.92
Pd NPs	40.221	2.244	2.7490	0

Table S3. Comparisons of EOR mass activity of AuPdCu NPs with other recently reported Pd-based catalysts.

Electrocatalyst	**Electrolyte**	**Scan rate ($mV \cdot s^{-1}$)**	**Mass Activity ($A \cdot mg_{Pd}^{-1}$)**	**Reference**
PdWNb/C	1 M KOH+1 M EtOH	50	15.6	[1]
PdCu	1 M KOH+1 M EtOH	50	10.78	[2]
Te-Pd NSs/C	1 M KOH+1 M EtOH	50	10.0	[3]
N-Pdene	1M KOH+1 M EtOH	20	7.96	[4]
AuPdCu NPs	1 M KOH+1 M EtOH	50	6.89	This work
Au@PdCore	1 M NaOH+1 M EtOH	50	6.83	[5]
PdCu SMPs	1 M KOH+1 M EtOH	50	6.09	[6]
PdAuCuNi NWs	1 M KOH+1 M EtOH	50	5.14	[7]
PdPtNi PNS	1 M KOH+1 M EtOH	50	5.12	[8]
Pd-$Ni(OH)_2$	1 NaOH+1 M EtOH	50	4.98	[9]
PdNiP	1 M NaOH+1 M EtOH	100	4.95	[10]
PdNi	1 M KOH+1 M EtOH	50	4.81	[11]
FA-Pdene	1 M KOH+1 M EtOH	50	4.122	[12]
meso-PdBi nanocages	1 M KOH+1 M EtOH	50	3.56	[13]
Pd-B MNSs	1 M KOH+1 M EtOH	50	2.95	[14]
Au@Pd NRs	1 M KOH+1 M EtOH	50	2.92	[15]
Pd MNPs/C	0.1 M KOH+0.5 M EtOH	50	2.88	[16]
PdRu/TiO_2	1 M KOH+1 M EtOH	50	2.696	[17]
PdInMo	1 M KOH+1 M EtOH	50	2.668	[18]
Pd nanosheets	0.5 M KOH+0.5 M EtOH	50	2.45	[19]
Pd/NPCM	1 M KOH+1 M EtOH	50	2.237	[20]

Pd_3Tb/C	1 M KOH+1 M EtOH	50	1.999	[21]
TS-Pd/C	1 M KOH+1 M EtOH	50	1.846	[22]
Pd NPs@Ni SAC	1 M KOH+1 M EtOH	50	1.093	[23]
Pd-Sb RHs/C	0.5 M NaOH+0.5 M EtOH	50	0.71	[24]
$PdSn@SnO_x$	1 M KOH+1 M EtOH	50	0.495	[25]

Reference

[1] Qin, Y. N.; Huang, H.; Yu, W. H.; Zhang, H. N.; Li, Z. J.; Wang, Z. C.; Lai, J. P.; Lei, W.; Feng, S. H. Porous PdWM (M =Nb, Mo and Ta) trimetallene for high C1 selectivity in alkaline ethanol oxidation reaction. Adv. Sci. 2022, 9, 2103722.

[2] Ipadeola, A. K.; Abdelgawad, A.; Salah, B.; Abdullah, A. M.; Eid, K.; Interfacial engineering of porous Pd/M (M = Au, Cu, Mn) sponge-like nanocrystals with a clean surface for enhanced alkaline electrochemical oxidation of ethanol. Langmuir 2023, 39, 13830-13840.

[3] Wang, L. P.; Yu, Z. Y.; Yan, W.; Liu, L. B.; Wang, M. J.; Kong, Q. Y.; Hu, Z. W.; Geng, H. B.; Huang, X. Q.; Li, Y. H. Palladium chalcogenide nanosheets with p-d orbital hybridization for enhanced alcohol electro-oxidation performance. Appl. Catal. B Environ. 2024, 343, 123564.

[4] Xie, M. H.; Zhang, B. W.; Jin, Z. Y.; Li, P. P.; Yu, G. H. Atomically reconstructed palladium metallene by intercalation-induced lattice expansion and amorphization for highly efficient electrocatalysis. ACS Nano 2022, 16, 13715-13727.

[5] Zhou, X. C.; Ma, Y. B.; Ge, Y.Y.; Zhu, S. Q.; Gui, Y.; Chen, B.; Liao, L. W.; Yun, Q. B.; He, Z.; Long, H. W.; Li, L. J.; Huang, B.; Luo, Q. X.; Zhai, L.; Wang, X. X.; Bai, L. C.; Wang, G.; Guan, Z. Q.; Chen, Y.; Lee, C. S.;Wang, J. L.; Ling, C. Y.; Shao, M. H.; Fan, Z. X.;Zhang, H. Preparation of Au@Pd core-shell nanorods with fcc-2H-fcc heterophase for highly efficient electrocatalytic alcohol oxidation. J. Am. Chem. Soc. 2022, 144, 547-555.

[6] Lv, H.; Sun, L. Z.; Wang, Y. Z.; Liu, S.H.; Liu, B. Highly curved, quasi-single-crystalline mesoporous metal nanoplates promote C-C bond cleavage in ethanol oxidation electrocatalysis. Adv. Mater. 2022, 34, 2203612.

[7] Lv, H.; Guo, X. W.; Sun, L. Z.; Xu, D. D.; Liu, B. A universal strategy for fast, scalable, and aqueous synthesis of multicomponent palladium alloy ultrathin nanowires. Sci. Chi. Chem. 2020, 64, 245-252.

[8] Wang, D. D.; Zhang, Y. P.; Zhang, K. W.; Wang, X. M.; Wang, C. Q.; Li, Z. L.; Gao, F.; Du, Y. K. Rapid synthesis of palladium-platinum-nickel ultrathin porous nanosheets with high catalytic performance for alcohol electrooxidation. J. Colloid Interf. Sci. 2023, 650, 350-357.

[9] Yang, H.; Zhang, A. C.; Bai, Y. F.; Chu, M. Y.; Li, H.; Liu, Y.; Zhu, P.; Chen, X. L.; Deng, C. W.;Yuan, X. L. One stone two birds:unlocking the synergy between amorphous $Ni(OH)_2$ and Pd nanocrystals toward ethanol and formic acid oxidation. Lnorg. Chem. 2022, 61, 14219-14427.

[10] Chen, L.; Lu, L. L.; Zhu, H. L.; Chen, Y. G.; Huang, Y.; Li, Y. D.; Wang, L. Y. Improved ethanol electrooxidation performance by shortening Pd-Ni active site distance in Pd-Ni-P nanocatalysts. Nat. Commun. 2017, 8, 14136.

[11] Ipadeola, A. K.; Abdelgawad, A.; Salah, B.; Ghanem, A.; Chitt, M.; Abdullah, A. M.; Eid, K. Self-standing foam-like Pd-based alloys nanostructures for efficient electrocatalytic ethanol oxidation. Int. J. Hydrogen Energ. 2023, 48, 30354-30364.

[12] Xie, S. Q.; Fu, J. S.; Huang, Q.; Yang, W. H.; Yu, A.; Yan, Y.Y.; Li, Z. Y.; Peng, P.; Yin, Y. J.; Wang, H. N. Echegoyen, Luis.; Li, F. F. Electronic modulation and active site exposure using C_{60} fullerenolamine enable high-performance alcohol oxidation on Pd metallene catalysts. Angew. Chem. Int. Ed. 2025, 64, e202506044.

[13] Du, D. W.; Geng, Q. H.; Ma, L.; Ren, S. Y.; Li, J. X.; Dong, W. K.; Hua, Q, F.; Fan, L. L.; Shao, R. W.; Wang, X. M.; Li, C. L.; Yamauchi, Y. Mesoporous PdBi nanocages for enhanced

electrocatalytic performances by all-direction accessibility and steric site activation. Chem. Sci. 2022, 13, 3819-3825.

[14] Lv, H.; Sun, L. Z.; Xu, D. D.; Henzie, J.; Yamauchi, Y.; Liu, B. Mesoporous palladium-boron alloy nanospheres. J. Mater. Chem. A 2019, 7, 24877-24883.

[15] Chen, Y.; Fan, Z. X.; Luo, Z. M.; Liu, X. Z.; Lai, Z. C.; Li, B.; Zong, Y.; Gu, L.; Zhang, H. High-yield synthesis of crystal-phase-heterostructured 4H/fcc Au@Pd core-shell nanorods for electrocatalytic ethanol oxidation. Adv. Mater. 2017, 29, 1701331.

[16] Li, J.; Zhou, Z. Y.; Xu, H.; Wang, C.; Hata, S.; Dai, Z. X.; Shiraishi, Y.; Du, Y. K. In situ nanopores enrichment of Mesh-like palladium nanoplates for bifunctional fuel cell reactions: A joint etching strategy. J. Colloid Interf. Sci. 2022, 611, 523-532.

[17] Liu, X. H.; Ning, L. N.; Deng, M.; Wu, J. Y.; Zhu, A. M.; Zhang, Q. G.; Liu, Q. L. Self-recoverable Pd-Ru/TiO_2 nanocatalysts with ultrastability for ethanol electrooxidation. Nanoscale 2019, 11, 3311-3317.

[18] Guo, Q. Q.; Dou, J. J.; Yang, X. X.; Jiang, Z. T.; Wang, H.; Liu, Y. M.; Xie, H. J.; Li, X.; Construction of Multiphase Concave Tetrahedral PdInMo Nanocatalyst for Enhanced Alcohol Oxidation. Adv. Funct. Mater. 2024, 35, 2413937.

[19] Zhang, Y.; Zhu, X.; Guo, J.; Huang, X. Q. Controlling palladium nanocrystals by solvent-induced strategy for efficient multiple liquid fuels electrooxidation. ACS Appl. Mater. Interfacces 2016, 8, 20642-20649.

[20] Yao, C. X.; Zhang, Q.; Cheng, B.; Chen, Q. Q.; Wang, R. J.; Zhou, X. F.; Ren, Y.; Wei, F. C.; Zhang, M. Palladium nanoparticles anchored on MXene-based N-doped porous carbon nanosheets as an advanced electrocatalyst for ethanol oxidation. J. Alloys Compd. 2023, 953, 169983.

[21] Li, Q. Q.; Sun, X. L.; Yin, Z. J.; Du, Y. P.; Liu, J. C.; Luo, F. Synthesis of palladium-rare earth alloy as a high-performance bifunctional catalyst for direct ethanol fuel cells. Nano. Res. 2024, 17, 9525-9531.

[22] Liu, C.; Shen, Y.; Zhang, J. F.; Li, G.; Zhang, X. R.; Han, X. P.; Zhu, S. Z.; Chen, Y. N.; Deng, Y. D.; Hu, W. B. Multiple twin boundary-regulated metastable Pd for ethanol oxidation reaction. Adv. Energy Mater. 2022, 12, 2103505.

[23] Li, S.; Guan, A. X.; Wang, H. N.; Yan, Y. Q.; Huang, H. L.; Jing, C.; Zhang, L. J.; Zhang, L.J.; Zhang, G. F. Hybrid palladium nanoparticles and nickel single atom catalysts for efficient electrocatalytic ethanol oxidation. J. Mater. Chem. A 2022, 10, 6129-6133.

[24] Xu, B. Y.; Liu, T. Y.; Liang, X. C.; Dou, W. J.; Geng, H. B.; Yu, Z. Y.; Li, Y. F.; Zhang, Y.; Shao, Q.; Fan, J. M.; Huang, X. Q. Pd-Sb rhombohedra with an unconventional rhombohedral phase as a trifunctional electrocatalyst. Adv. Mater. 2022, 34, 2206528.

[25] Chandran, A. P.; Mondal, S.; Goud, D.; Bagchi, D.; Singh, A. K.; Riyaz, M.; Dutta, N.; Peter, S. C. In situ metal vacancy filling in stable Pd-Sn intermetallic catalyst for enhanced C-C bond cleavage in ethanol oxidation. Adv. Mater. 2024, 37, 2415362.